

4. Deposition Velocity

The general approach of estimating atmospheric deposition rates by using observed atmospheric concentrations in conjunction with theoretical deposition velocities is a well-established methodology (e.g., Brook et al. 1999; Smith et al. 2000, Wesely and Hicks, 2000; Lu et al. 2003). This section describes the estimation of the deposition velocities that are subsequently used to estimate the deposition of nitrogen, phosphorus, and particulate matter directly to the surface of Lake Tahoe. The ambient concentrations used in estimating atmospheric deposition are described in Chapter 3.

Deposition to land surfaces and subsequent transport to the Lake is outside the scope of LTADS; however, it is included in the watershed analysis for the TMDL process. Materials deposited on land and subsequently transported to the Lake will be included in estimates of other nutrient and sediment inputs such as stream flow and direct runoff to the Lake. These indirect atmospheric deposition estimates are being developed under the auspices of the Lahontan Regional Water Quality Control Board (RWQCB). Lahontan RWQCB is also estimating inputs from streambed erosion, shoreline erosion, and ground water exchange. The TMDL process will utilize the estimates of atmospheric deposition to the Lake surface, provided by LTADS, and estimates of inputs of nutrients and sediment via other mechanisms, provided by Lahontan RWQCB and their contractors.

For several reasons, the relative contribution of deposition to land areas with subsequent transport to the Lake is expected to be small relative to that in other watersheds. First, some of the nutrients deposited over land would be assimilated before reaching the Lake. Second, the ratio of Lake area (500 km²) to land area (800 km²) exceeds that of many watersheds. Third, the high proportion of natural surfaces at Tahoe increases percolation and decreases runoff of precipitation compared to more urbanized areas.

Estimation of wet deposition, meaning deposition of aerosols or gases contained within rain, snow, or other precipitation, is a separate topic and utilizes different methods. Estimates of wet deposition to the Lake will likely be based upon samples of total deposition (wet and dry) collected at buoys on the Lake during periods dominated by precipitation.

Note that the calculation of dry deposition provided here assumes that dry deposition processes are in effect continuously during each hour and day throughout the year, irrespective of whether or not there is any precipitation. This is one of several assumptions that are intended to provide a conservatively large estimate of dry deposition.

4.1 Meteorological Context

Because population, roads, and other activities that generate emissions in the Tahoe Basin are generally located near the shore of the Lake, the daily patterns of airflow are

important to spatial variations in concentrations and source-receptor relationships. In addition, the wind direction affects the deposition velocity over the near-shore waters. With an offshore wind direction (i.e., from the shore toward the Lake) larger surface roughness elements (e.g., trees and buildings) cause more turbulence than with an onshore wind direction (i.e., from the Lake toward the land). Sun, et al. (2001) examined direct (eddy covariance) observations of the turbulent transport of momentum in a coastal zone and found evidence that turbulence generated by on-land surface roughness elements was advected over the water. The resulting increase in vertical transport of momentum extended for a distance of a few kilometers offshore. This phenomenon also affects deposition velocities at Lake Tahoe, although wind speeds at Tahoe are lower than those observed by Sun so that downwind over-water influences of surface roughness may be less spatially extensive than in the coastal case.

At Tahoe, wind speed and direction typically vary in predictable daily patterns as a result of the altitude, terrain, and thermal inertia of the Lake. The thinner and often drier atmosphere at higher altitudes causes larger day-night swings in land surface temperatures at Tahoe than sea-level locations. However, this tendency toward large temperature swings is for land surfaces only. The temperature of the Lake surface is moderated by the large thermal mass of the deep Lake so that the water maintains a more constant surface temperature.

The resulting difference in air temperatures over the land and Lake cause well-organized mesoscale winds. The locally generated mesoscale winds operate in conjunction with the regional flows. In the Tahoe Basin, the regional airflow is generally from the southwest or west, shifting to the south before storms and to the northwest or north after storms. The interaction of regional flows and mesoscale lake-land breezes were analyzed in detail by Sun, et al. (1997) based upon extensive observations of meteorological variables and fluxes obtained over Candle Lake during the Boreal Ecosystem Atmosphere Study (BOREAS).

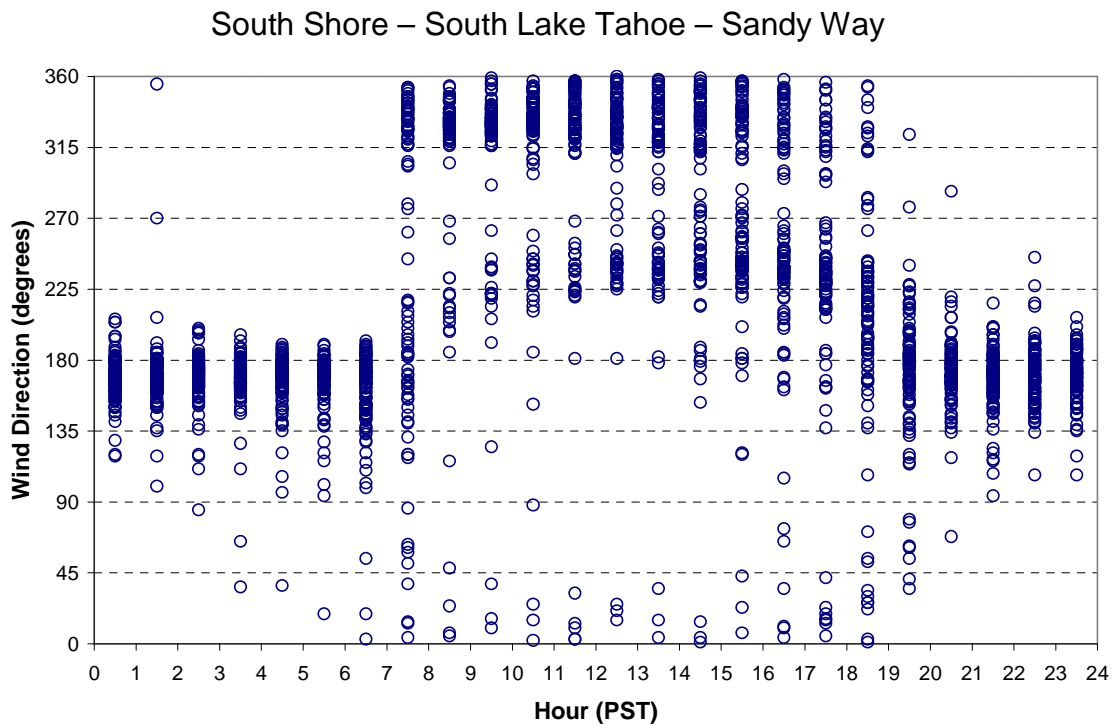
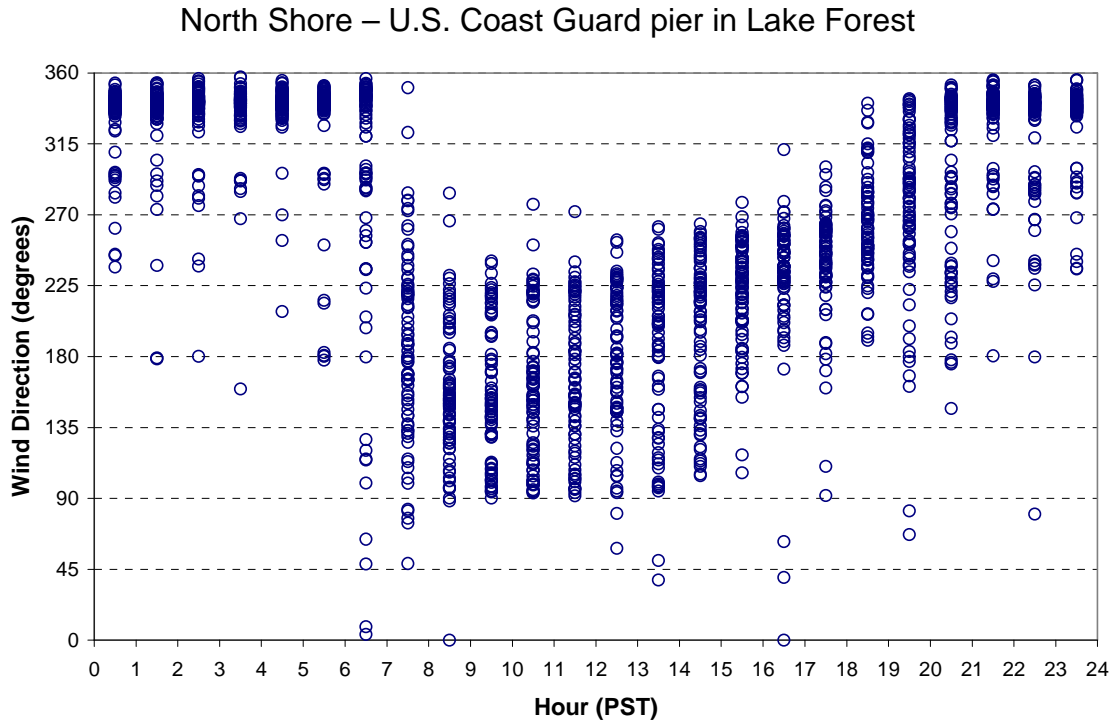
Over sloping terrain, the nighttime cooling and daytime heating of air near the surface causes shallow density-driven flows, up-slope during the day and down-slope during the night and early morning. Thus, the wind speed and direction, especially near the surface, tend to vary with time of day in a predictable way. The influence of local temperature differences also causes local pressure gradients that generate winds at higher altitudes. For example, for many hours of the year (at night and during winter) the Lake water is warmer than the air advected over it. Air at the surface of the water is warmed and mixes upward a few or many hundreds of meters above the surface of the Lake. The resulting differences in air density create local pressure gradients that affect the wind directions from the surface to well above the height of the mixed layer over the Lake. There may be offshore winds at the surface with return flow from lake toward land at higher altitudes.

As an illustration of the importance of these mesoscale patterns, the diurnal variation in wind direction during the summer of 2003 is plotted for a north-shore and a south-shore surface location in Figure 4-1. The winds at any given time of day tend to be in

opposing directions at the two locations. The direction the wind is coming from is shown in degrees, where 0 or 360 degrees indicate wind from the north, 90 degrees indicate wind from the east, 180 degrees indicate wind from the south, and 270 degrees indicate wind from the west. Comparing the two plots, winds are down-slope during the night (from the NNW at the north-shore and SSE at the south-shore), abruptly shift to up-slope after sunrise (SE through SW at north-shore and NW at the south-shore), and transition back to down-slope flow after sunset. The up-slope/down-slope airflow is quite evident at all monitoring sites around the Lake during all seasons of the year, although migrating storm/low pressure systems during the winter and spring disrupt the pattern.

Deposition velocities for gases and particles were modeled for each hour of 2003 for which data were available using meteorological data (wind direction, wind speed, air temperature, and water temperature) observed at buoy and pier locations. The meteorological measurements were made at heights of 5 to 7 m above water level on the piers and 3 m above water level on buoys. Water temperature was measured at the 2-cm depth. The ambient concentrations, which are paired with the calculated deposition velocities, were measured at the land-based monitoring sites, which were generally located near the shoreline. The inlet of the TWS was 2.1 m above ground level for all sites, except at Sandy Way where the inlet was 2.1 m above the flat roof of the one-story building.

Figure 4-1. Diurnal Profiles of Wind Directions during summer 2003 at North Shore and South Shore Locations on Lake Tahoe



4.2 Calculation of Deposition Velocity and Resistances for Gases

As noted in Section 2, the dry deposition rate is modeled as the product of concentration and deposition velocity, integrated over a variety of gaseous species and spectrum of particle sizes, over time, and across the area of the Lake surface.

The “deposition velocity” (V_d) is the rate of deposition or flux (F), with units of mass/area/time) divided by the difference in concentrations in the well-mixed atmosphere (C) versus air at the surface where removal takes place (C_0).

$$V_d = F / (C - C_0) \quad (4.1)$$

In many cases C_0 equals or approaches zero so that the deposition rates, or flux (F), of a compound equals or can be approximated by:

$$F = V_d * C \quad (4.2)$$

Thus, the deposition velocity is the deposition rate normalized for concentration, providing a measure of the environmental propensity for atmospheric deposition independent of ambient concentration. Although it has units of velocity (distance/time, usually expressed in cm/sec), it does not describe a physical process or velocity.

Estimation of V_d requires consideration of the controlling processes that comprise it. V_d is commonly estimated using a model of resistances or conductances analogous to electrical circuitry. For gases, the total resistance to transfer (R_{total}) is the sum of three basic resistances acting in series (see Figure 4-2). These are the aerodynamic resistance (R_a), the “quasi-laminar” boundary layer (or viscous sub-layer) resistance (R_b), and the surface (or vegetation canopy) resistance (R_c).

R_a is the resistance to mixing through the boundary layer toward the surface by means of the dominant process, turbulent transport. A large value of R_a would indicate a relative lack of turbulence.

The quasi-laminar layer resistance, R_b , is resistance to movement across the thin layer (0.1 – 1 mm) of air that is in direct contact with a surface and not moving with the mean flow of the wind. Through this thin layer, in the absence of turbulence, the primary transport process for gases is molecular diffusion. For gases the quasi-laminar layer resistance is designated as R_b . For particles the important transport processes in this layer are Brownian motion and inertial impaction). To differentiate from gases, the quasi-laminar layer resistance for particles is designated as R_d . R_c , the resistance of a compound to uptake by a surface, varies both with the surface and the chemical species or physical state (gas or particle). For gases the deposition velocity can be expressed as:

$$V_d = 1/(R_a + R_b + R_c) \tag{4.3}$$

Highly reactive and highly soluble gases, such as nitric acid and ammonia are readily deposited to water surfaces and so, over water, their values of R_c (and C_0) are essentially zero. For gases in general we have also assumed that $R_a \gg R_b$. Thus, equation 4.4 for gases is simplified as:

$$V_d = 1/R_a \tag{4.4}$$

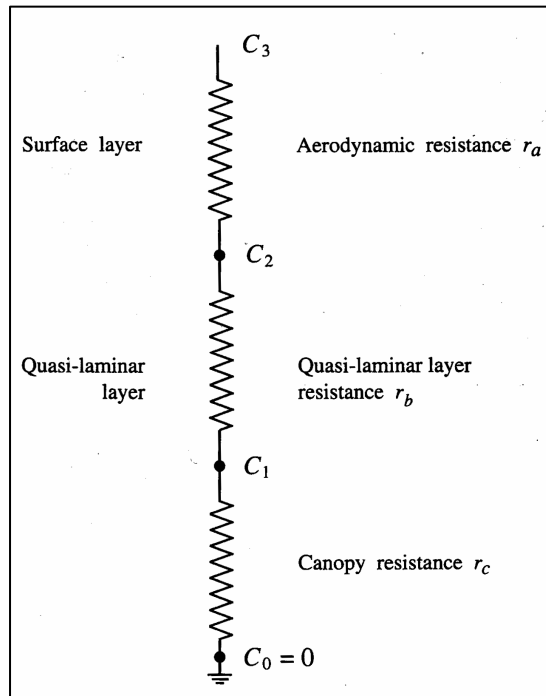


Figure 4-2. Resistance model for dry deposition of gas.

Source: <http://www.atmosp.physics.utoronto.ca/people/ulrike/lecture-notes/Lecture3.ppt>

For deposition of particles it is necessary to calculate R_d . It is also necessary to consider a gravitational settling which is parallel path for deposition that is not shown in Figure 4-2. Gravitational settling is generally important for larger particles, i.e., with particle diameter (D_p) $\gg 1 \mu\text{m}$. Following detailed discussion of the calculation of aerodynamic resistance, R_a , the calculation of the quasi-laminar layer resistance for particles, R_d , and the gravitational settling of particles will be presented.

4.2.1 Calculation of Aerodynamic Resistance (R_a) for gases and particles

The aerodynamic resistance, R_a , is controlled by the level of atmospheric turbulence available to transport gases and particles in the air into close proximity to the surface. This section describes methods for calculation, including one that is under consideration

for future work but was not applied here. All require estimation of the Monin-Obhukov Length (L) scale, which is a stability parameter. Also discussed at the end of section 4.2.1 are estimation of the aerodynamic roughness length (Z_o) and assumptions about the variation in wind speed with height through the surface layer.

Definition of Aerodynamic Resistance

A commonly used formulation for aerodynamic resistance assumes similarity between turbulent transport of chemical species and turbulent transport of momentum. That formulation is:

$$R_a = U / (U^*)^2, \quad (4.5)$$

where U is the wind speed and U^* (pronounced Ustar) is the friction velocity. The friction velocity is a measure of the shearing stress of the wind on the surface below. It is defined as the square root of the surface shear stress divided by the density of air. Methods used to estimate U^* are provided in the following sections. The wind speed is usually directly measured. Although friction velocity may be determined by direct measurement of momentum flux by the eddy covariance (EC) method, friction velocity is less exactly but commonly estimated from more routine meteorological measurements of wind speed and temperature at multiple heights.

Primary Calculation of Aerodynamic Resistance

LTADS calculated the friction velocity and aerodynamic resistance using the formulation of Byun and Dennis (1995) adapted for use over water. The relationship of wind speed (U_z) to height above the surface (z) is the logarithmic profile adjusted for stability of the atmosphere as described by the Monin Obhukov Length scale (L). The form of the equation depends on the sign of L.

For the stable atmosphere case, where $L > 0$ (based on $T_{air} > T_{water}$),

$$U_z = [(U^*)/(k)] * [\ln((z - Z_o)/ Z_o) + 4.7 * (z/L)], \quad (4.6)$$

where:

k = Von Karmen constant = 0.4

Z_o = aerodynamic roughness length

U^* = friction velocity. The square of the friction velocity equals the wind-induced shear stress at the surface divided by density of air.

For the unstable atmosphere case, where $L < 0$ (based on $T_{air} < T_{water}$),

$$U_z = [(U^*)/(k)] * [\ln(\text{numerator}/\text{denominator})], \quad (4.7)$$

where:

$$\begin{aligned} \text{numerator} &= [(1 + 16 * z / |L|) - 1]^{1/2} * [(1 + 16 * Z_o / |L|) + 1]^{1/2} \\ \text{denominator} &= [(1 + 16 * z / |L|) + 1]^{1/2} * [(1 + 16 * Z_o / |L|) - 1]^{1/2} \end{aligned}$$

The formulation of Monin-Obhukov Length scale (L) used here is that of Hanna, et al. (1985) which is used in the meteorological model CALMET (Scire, et al., 2000a) for calculation of momentum flux over water.

$$L = (T_a + 273.16) [((0.75 + (0.067)(U_{10}))/1000)]^{3/2} / [(E2)(T_a - T_w)] \quad (4.8)$$

where:

- T_a is the observed air temperature
- U₁₀ is the wind speed extrapolated to 10 meters
- T_w is the observed water temperature
- E2 = 0.0051

Differences between the subsurface water temperature and the near surface air temperature may be a source of bias; however, the formula applied here is designed and intended for use with water temperature.

The formulation of aerodynamic roughness length (Z_o) over water is from Hosker, (1974) and takes the following form.

$$Z_o = (0.000002)(U_{10})^{5/2} \quad (4.9)$$

As discussed at the end of section 4.2.4, near the shoreline the value of Z_o also depends strongly upon wind direction and this was taken into account in the iterative solution.

In the absence of resource intensive direct measurements of the friction velocity (U*), the value of U* can be calculated from the wind speeds and temperatures observed at two or more heights. By using an iterative method it is also possible based water temperature and meteorological observations at a single height to calculate the values of friction velocity (U*), aerodynamic roughness length (Z_o), and Monin-Obhukov Length scale (L). Multiple iterations are needed because of the interdependence of these variables.

LTADS used an iterative solution in which Z_o and L were estimated using formulations that require input of an estimated wind speed at 10 meters (U₁₀). For initial estimates of Z_o and L the wind speed at the instrument height was substituted for wind speed U₁₀ in equations 4.8 and 4.9. Successive estimates of U₁₀ were made with equations 4.6-4.7 and Z_o and L were recalculated upon each new estimate of U₁₀. Note that the equations 4.8 and 4.9 are specific to applications over water.

From equations 4.5 and 4.6-4.7 the aerodynamic resistance, R_a, takes the following forms. For the stable atmosphere case, where L > 0 (based on T_{air} > T_{water}),

$$R_a = [1/(k * (U^*))] * [\ln(z/ Z_o) + 4.7 * (z/L)], \quad (4.10)$$

For the unstable atmosphere case, L < 0 (based on T_{air} < T_{water}),

$$R_a = [1/(k * (U^*))] * [\ln(\text{numerator}/\text{denominator})], \quad (4.11)$$

where:

$$\begin{aligned} \text{numerator} &= [(1 + 16 * z / |L|) - 1]^{1/2} * [(1 + 16 * Z_o / |L|) + 1]^{1/2} \\ \text{denominator} &= [(1 + 16 * z / |L|) + 1]^{1/2} * [(1 + 16 * Z_o / |L|) - 1]^{1/2} \end{aligned}$$

4.2.2 Bulk Calculation of Momentum Flux and Friction Velocity

For the purpose of a rough comparison, LTADS also estimated the aerodynamic resistance from equation (4.5) using a bulk coefficient method to get the friction velocity. This method is applied in the CALMET model (Scire, et al., 2000) for estimation of momentum flux over water.

The friction velocity, U^* , is calculated in m/s as by Garrat, et al. (1977):

$$U^* = U_{10} (C_{UN})^{1/2}, \quad (4.12)$$

where the bulk coefficient, C_{UN} is given by:

$$C_{UN} = (0.75 + 0.67 * U_{10}) / 1000, \quad (4.13)$$

R_a is then calculated from equation 4.5 in units of s/m or in units of s/cm as

$$R_a = [(U_{10}) / (U^*)^2] / 100, \quad (4.14)$$

However, for this comparison, the observed wind speeds were not extrapolated to 10 meters due to time constraints. Instead, wind speeds at instrument height were substituted directly in place of U_{10} in equations 4.12-4.14 (omitting the step of extrapolating the wind speeds, from instrument heights (of 3 m above the Lake surface on buoys and 5 to 7 m above the Lake surface on piers) to a 10-m reference height). Thus, wind speeds were underestimated in equations 4.12-4.14 and the resulting estimates of the aerodynamic resistance (R_a) were slightly higher and estimates of deposition velocities (V_d) were slightly lower than if an extrapolated value of U_{10} was used. than with the formulation of Byun and Dennis described in section 4.2.1.

4.2.3 Alternative Method Not Utilized

Valigura (1995) modeled deposition of HNO_3 , making the common assumption that $R_a \gg R_b$. He assumed similarity between turbulent transport of heat and chemical species for calculation of R_a . Heat flux was modeled by iterative solution of a surface energy balance. To verify the model, Valigura compared measured and modeled values of skin temperature and heat flux. The results were reported to be inconclusive and differences, between measured and modeled values, were attributed to a possible mismatch in scales of observations obtained with aircraft-based and boat-based instruments.

For completeness and comparison with the current results, it may be possible to make calculations by an adaptation of Valigura's method. That would require measurements or a parameterization of net radiation suitable for the altitude of Lake Tahoe and availability of meteorological (e.g., cloud type and height) data. However, adequate data for verification of the modeling may not be available and it is not clear that the work could be completed within the timeframe available for releasing the final report. If the

method were applied, observations of water skin temperature would be very useful for verification, but such data are not currently available.

Some radiometric measurements of water skin temperature may potentially be available from other sources. We are seeking such data from UC Davis and NASA scientists who have made some water skin temperature measurements from piers and buoys. It is unlikely that any satellite-based observations could become available in time for our use due to the labor intensive requirements for processing the raw data.

Verification of Estimates

Modeling estimates of either momentum flux or heat flux could be validated against direct measurements by the eddy covariance (E-C) method.

Although not collected as part of LTADS, some eddy covariance measurements of momentum flux, heat flux, sensible heat flux, and friction velocity are available from experiments at Lake Tahoe and elsewhere. Use of these data would require quality assurance analyses first, but they could allow better estimates of the uncertainty in the values of aerodynamic resistance that are predicted using the methods discussed above.

Restrictions on Assumption of Log Wind Profile

The formulations used here to estimate R_a assume a logarithmic wind profile, but this assumption is not valid for heights of less than 50 times the aerodynamic roughness length (Brutsaert, W., 1982). The following sections describe estimation of the aerodynamic roughness length (Z_o) and implications for calculations involving measurement heights or reference heights of less than $50 * Z_o$.

4.2.4 Treatment of Aerodynamic Roughness Length, Z_o

The aerodynamic roughness length scale, Z_o , represents the effects of surface roughness on the wind flow as that roughness affects the generation of shear induced turbulence. The aerodynamic roughness length is defined as the height at which the horizontal wind speed goes to zero. It is not equal to the height of individual roughness elements, but there is a one-to-one correspondence between these roughness elements and the aerodynamic roughness length. The amount of downwind turbulence generated by wind flow over a rough surface is a factor in determining the vertical profile of wind speed and the aerodynamic resistance, R_a . Z_o is used to represent this effect in the equations of the vertical profile of wind speed, momentum flux, and aerodynamic resistance. Particularly for larger values of Z_o , the aerodynamic resistance and the deposition velocity are sensitive to Z_o .

Over open water, the shear force of the wind causes waves to develop and Z_o is commonly estimated as a function of either friction velocity or wind speed. Various formulations are available dating from the classical formulation by Charnock (1955) to the formulation used here (Hosker, 1974) that was presented as equation 4.9. This calculation of Z_o is also used near shore when the wind direction is onshore (from Lake toward land).

When the wind direction is offshore (from land to water), there is advection of greater turbulence associated with greater surface roughness elements over land as was observed by Sun (2001) in coastal environments. The effect is to decrease aerodynamic resistance and increase deposition velocity in the near-shore zone when the wind is offshore. This effect is implemented by making separate calculations for offshore wind direction and onshore wind direction. During offshore flow, to represent conditions at the shoreline (and at the piers where the meteorological measurements are made) the aerodynamic resistance is calculated using an aerodynamic roughness length of 1 meter to characterize the effects of the land area immediately upwind. This value of Z_o , for offshore wind direction, in turn affects the calculation of the friction velocity and extrapolation of the wind speed to 10-meters above the surface. The result is to decrease R_a and increase deposition velocity. The advection of turbulence from over land is assumed to affect the aerodynamic resistance from the shoreline to a distance of 1 km offshore. The computations assume a linear decay of the near-shore R_a to the open-water R_a at a distance of 1 km offshore.

4.2.5 Assumption of Logarithmic Wind Profile

Estimation of R_a by either of the methods described above assumes the wind speed increases with the logarithm of height. However, that assumption (of a logarithmic wind profile) is not theoretically valid at heights less than 50 times the aerodynamic roughness length, Z_o (Brutsaert, 1982). Over open water and in the near-shore zone with onshore flow, the Z_o is sufficiently small, on the order of 0.0001 m, that assumption of the log wind profile is reasonable at heights well below the heights of wind observations. However, with offshore winds, the larger surface roughness elements over land affect the flow over the near-shore waters increasing the aerodynamic roughness length to 1 or 2 meters, so that the assumption of a log wind profile is not satisfied near the surface. Even with a moderate assumption of $Z_o = 1$ m in the vicinity of the pier mounted meteorological instruments, the assumption of a logarithmic wind profile at the measurement heights of less than 10 meters is thus not theoretically valid. This constraint is widely ignored in the literature, largely because little error is introduced for most uses of the logarithmic profile. But this turns out not to be the case for the calculation of the aerodynamic resistance.

The calculated values of R_a are inordinately sensitive to Z_o when Z_o is of the same order of magnitude as the observation height Z . For this situation the calculated values of R_a were unreasonably small and the resulting estimates of deposition velocity were unrealistically large. This was remedied by setting a lower limit of 1/6 s/cm for R_a . When calculating deposition velocity for gases, this sets an upper limit of 6 cm/s on V_d . Selection of this particular value was based on literature indicating the maximum observed deposition rates over water for another reactive soluble gas (SO_2) are in the range of 3 to 4.5 cm/s and a desire, consistent with the LTADS purpose, to provide upper-limit, conservative estimates of deposition velocities and deposition rates. The lower limit of 1/6 s/cm for R_a and resulting upper limit deposition velocity of 6 cm/s for gases was invoked for many of the hours of offshore flow but was not invoked for mid-Lake or for near-shore areas during onshore flow. Thus, this limit is only applied in the

near-shore region when larger values of Z_o are applied for offshore flow. The near-shore region affected by advection of increased turbulent kinetic energy generated by flow over larger roughness elements was estimated to extend 1 km from shore and to comprise 20 percent of the surface area of the Lake.

4.2.6 Boundary Layer Resistance (R_b) for gases and (R_d) for particles

R_b is resistance to transport through the very thin (0.1 – 1 mm) viscous sub-layer at the surface. This layer is also referred to as the quasi-laminar layer (Hicks, 1982) or the laminar deposition layer (Scire et al., 2000a). The quasi-laminar resistance (R_b) for gases is differentiated from the quasi-laminar resistance for particles (R_d). Transport through this thin layer is by molecular diffusion for gases and by Brownian motion and impaction for particles. For gases R_b is generally considered to be very small compared to R_a . However for estimating the deposition velocity of particles, R_d must be explicitly calculated. Because the quasi-laminar layer resistance for particles (R_d) and the particle gravitational settling velocity (V_g) require some of the same variables, the formulas for their calculation are grouped in section 4.3.1

4.2.7 Surface Resistance (R_c)

The surface resistance of water is very small (effectively 0) for both particles and highly reactive or soluble gases such as nitric acid or ammonia. However, the relative contribution of nitrogen to the Lake by deposition of other gaseous N species, such as NO_2 , is very small because R_c is a large limiting resistance and the deposition velocity is very small. Although LTADS is not estimating deposition over land surfaces, it may be of interest that for moderately reactive chemical species, such as ozone or NO_2 , the surface resistance, R_c , over land varies spatially with differences in land use and vegetation type and temporally with biophysical responses of vegetation to light, moisture, etc.

4.3 Deposition of Particles

For estimating deposition velocities for particles, gravitational settling velocity, V_g , must be considered in addition to the resistances discussed above. The gravitational settling velocity, V_g , is mainly important for larger particles.

Transport through the thin quasi-laminar layer is by Brownian motion and impaction for particles. The primary mechanism is Brownian motion for fine particles, and impaction for larger particles (of $D_p \gg 1 \mu\text{m}$). The quasi-laminar layer resistance for particles, R_d , is greatest for particles in the size range of $D_p \sim 0.3\text{-}0.5 \mu\text{m}$ because the rates of Brownian diffusion and impaction for these particle sizes are both low. For this size range, R_d over water can be a primary constraint to deposition causing a minimum in V_d for accumulation mode particles. A representation of the effects of particle size on deposition velocity is shown in Figure 4-3.

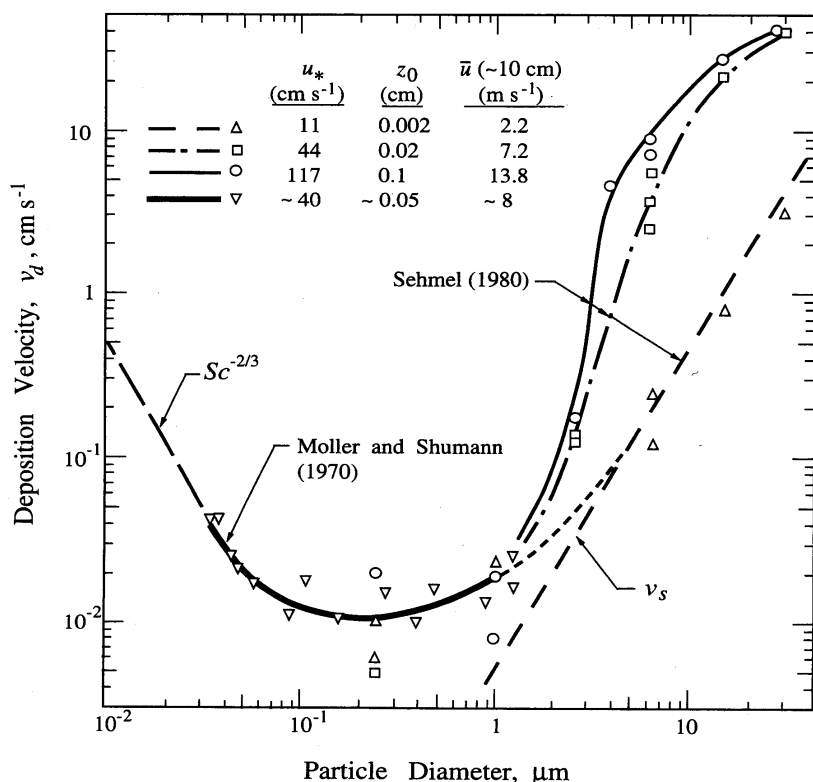


Figure 4-3. Deposition velocity is a non-linear function of particle size.
 Source: <http://www.atmosp.physics.utoronto.ca/people/ulrike/lecture-notes/Lecture3.ppt>

4.3.1 Traditional Formulation of Particle Deposition Velocity

In equations 4.1 - 4.4 and figure 4.2 we presented the general model for deposition of gases. The analogous model for deposition of particles is described in equation 4.15 (or equation 4.18) and figure 4.3. The formulation of particle deposition common to many current air quality models (e.g., CALPUFF and ISCST3) was used by LTADS. Many authors, e.g., Slinn and Slinn (1980), Pliem et al. (1984), and Seinfeld and Pandis (1998) have presented this general form shown below.

$$V_d = V_g + [1/(R_a + R_d + R_a * R_d * V_g)] \tag{4.15}$$

The gravitational settling velocity, V_g , is not simply additive because it is a parallel path in competition with the path shown in Figure 4-2. The equations for the gravitational settling velocity, V_g , and quasi-laminar layer resistance, R_d , are given below along with additional variables used in their calculation. Note that the formulation for the aerodynamic resistance, R_a , is that of Byun and Dennis, which was presented previously and is applicable to either particles or gases.

The quasi-laminar layer resistance parameterizes the effects of Brownian motion and inertial impaction of particles as the means of transport through the quasi-laminar layer. Thus, the quasi-laminar resistance for particles (R_d) is analogous to but differentiated from the quasi-laminar layer resistance for gases (R_b) which parameterizes molecular diffusion.

$$R_d = (1/(U_*)) / (Sc)^{-2/3} + 10^{-3/St}, \quad (4.16)$$

where:

Sc = Schmidt number = V_a / D_b , where:

V_a = viscosity of air = $0.15 \text{ cm}^2/\text{s}$

D_b = Brownian diffusivity (cm/s) = $8.09 * (T_a + 273.16) * 10^{-10} * Sc_f/\text{diam_pm}$,

where:

Scf = Cunningham slip correction factor

= $1 + (2 * x_2) * (a_1 + a_2 * \exp^{-a_3 * \text{diam_pm}/x_2}) / (\text{diam_pm} * 0.0001)$,

where:

$x_2 = 0.0000065$

$a_1 = 1.257$

$a_2 = 0.4$

$a_3 = 0.000055$

diam_pm = measured, or assumed, diameter of particle

St = Stokes number = $(V_g/a_g) * (U_*)^2 / V_a$, where:

a_g = acceleration due to gravity (981 cm/s^2)

The gravitational settling velocity, V_g , was introduced previously. It is primarily dependent of particle size and density. In units of (cm/s) it is calculated as:

$$V_g = [(\rho_p - \rho_a) * a_g * [\text{diam_pm}]^2 c_2] * Sc_f / (18 * V_a), \quad (4.17)$$

where:

ρ_p = density of particle; value input ($\sim 1\text{-}3 \text{ g/cm}^3$)

ρ_a = density of air (g/cm^3)

= $0.012 * [(T_a + 273.16)/273.16] * (P_a / 1000)$,

where:

P_a = atmospheric pressure (mb)

$c_2 = 0.00000001 \text{ cm}^2/\text{mm}^2$

4.3.2 Correction to Formulation of V_d for Particles

Although the basic formulation, equation (4.3), is still widely applied, Venkatram and Pleim (1999) showed that it violates the fundamental physical constraint of mass conservation. Alternatively, they derived a formulation satisfying that constraint:

$$V_d = V_g/[1 - e^{-V_g(R_a + R_d + R_c)}] \quad (4.18)$$

The final LTADS report will compare the results provided by both formulations. However, as the authors have suggested, the deposition velocity estimates from the corrected formulation are likely to differ only for a limited range of particle sizes. Thus, any changes in estimated deposition rates with use of the more current and defensible formulation are expected to be minor.

4.4 Key Assumptions and Resultant Bias

Identified in this section are key assumptions used in the estimation of deposition velocities and, subsequently, pollutant deposition. They are segregated based upon whether we expect them to introduce a positive bias in the estimates of deposition velocity or whether, based on the available information, the likely sign of the bias is unknown. Some assumptions clearly will introduce a significant positive bias. This was intentional in the hopes of avoiding any future upward adjustment of the deposition estimates upon the completion of more refined analyses.

4.4.1 Assumption Likely Introducing the Largest Positive Bias

The assumption that concentrations measured on land, near emission sources are representative of concentrations over mid-Lake areas is expected to introduce a significant positive bias in the estimated deposition rates.

Use of this assumption will overestimate concentrations and deposition rates for several reasons. First, the monitoring sites are relatively close to emission sources and dispersion will decrease the downwind concentrations of all sizes of particles. Second, deposition will also decrease the mass concentrations downwind. Third, deposition will preferentially decrease concentrations of larger particles. The remaining smaller particles will have a smaller deposition velocity.

4.4.2 Assumptions Likely to Introduce a Moderate Positive Bias

Deposition velocity was estimated for each hour for which the meteorological data were available. The calculation of seasonal and annual deposition assumes that dry deposition occurs during every hour, including wet periods, thus, creating a positive bias by over counting the hours of dry deposition.

Assumptions regarding characteristic particle size within each of three size bins are likely to introduce a moderate positive bias for estimates of the upper bound deposition rates of particles. The particle size assumptions utilized for lower bound, best, and upper bound estimates of deposition rates (summarized in section 5-6) are defined below and are followed by background information including observed particle sizes.

For calculating deposition velocities representative of each PM size category, a lower bound, a best estimate, and an upper bound set of values were assumed for the mass-weighted representative particle diameters (i.e., above the lowest possible size for the lower bound calculation, above the mid-point of the size distribution for the best estimate calculation, and at or near the most extreme particle size possible for the upper bound calculation):

- Characteristic sizes of PM-fine (PM diameter < 2.5 μm) were set at 1, 2, and 2.5 μm . Clearly, PM-fine must include particles smaller than 2.5 μm and the assumption of 2.5 μm as the characteristic size must overestimate the actual deposition velocity.
- Characteristic sizes of PM-coarse (2.5 μm < PM diameter < 10 μm) were set at 5, 8, and 10 μm . Similarly, 10 μm must overestimate the characteristic size of PM-coarse and thus the deposition velocity.
- Characteristic sizes of PM-large (10 μm < PM diameter < 25 μm \leq TSP) were set at 15, 20, and 25 μm . There is no upper limit defined on the size of PM-large, but, as detailed in the section above, the available data suggests that 25 μm is an overestimate of the characteristic particle size of PM-large, and thus will overestimate the actual deposition velocity. Thus, there is reasonable certainty that the assignment of 25 μm as the characteristic size for large particles is sufficiently conservative to represent the worst case condition at the shoreline of the Lake. Applying these same particle sizes for calculations at mid-Lake should be yet more conservative as an upper bound of deposition to the Lake.

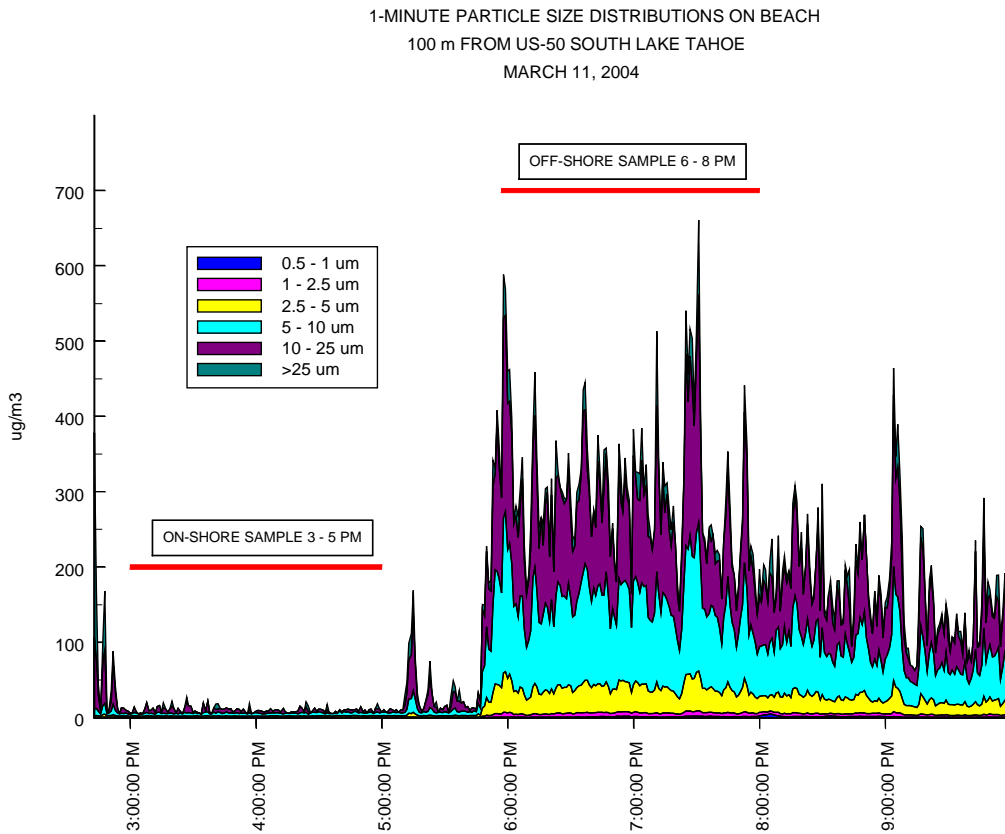
Although larger particle sizes have been observed in urban areas of southern California by Lu, et al. (2003), we conclude from the available LTADS data that particles larger than 25 μm contribute a relative small fraction of the mass of particles larger than PM10 over Lake Tahoe. This conclusion is based on the TWS data and short-term observations with optical particle counters that provide additional size resolution.

Short-term experiments were conducted in which particle counts were measured in five size bins at multiple locations between the lakeshore and primary roadways encircling the Lake. The particle counts were converted to relative mass concentrations by assuming that particle densities were uniform among different sizes. Figure 4-4 shows a time series of the estimated mass concentrations in five size bins as observed in early spring during onshore and offshore flow at the beach near the SOLA site, about 100 meters from Highway 50. From 3 to 5 PM with the wind coming off the Lake, the concentrations were relatively low. After a typical late afternoon wind shift to down-slope (offshore) flow, concentrations estimated from the particle counter, which was downwind of Highway 50, increased very substantially.

The mass concentration of PM2.5 particles is barely discernable compared to the much larger concentration of the PM-coarse particles, which encompasses two size cuts, 2.5 - 5 μm (yellow) and 5 - 10 μm (turquoise). The PM-large particles also encompasses two size cuts, 10 - 25 μm (purple) and > 25 μm (red) but the mass concentration of PM > 25 μm is relatively small. The concentrations of PM-large (>10 μm) was less than that of PM-coarse (2.5 < diameter < 10 μm).

Within the size category of PM-large, relative mass concentrations can be compared between two size bins, particles of diameter less than or greater than 25 μm . In Figure 4-5, the mass distributions by size bin are shown as integrated for two-hour periods of onshore flow (dashed line) and offshore flow (solid line). Using a log concentration scale facilitates viewing the relative concentrations from each of the size bins, including those with smaller concentrations. The relative mass of PM >25 μm is less than about

Figure 4-4. An optical particle counter was located on the beach in South Lake Tahoe approximately 100 m from Highway 50 during light onshore (3-5 PM) and light offshore (6-8 PM) winds. From the optical counts, mass concentrations are estimated for five size categories, assuming spherical particle shape and equal density for all particle sizes. Estimated mass is only approximate but considered suitable for demonstrating the relative mass of particles in each size category.



10% of the PM > 10 μm mass when the particle counter was downwind of the roadway, and less than 2% when downwind of the Lake.

Although the TWS does not resolve differences in size for particles larger than 10 μm , it likewise provides supporting evidence that the mass of large particles is dominated by particles smaller than 25 μm . With only relatively small differences observed between the concentrations of PM10 and TSP and without a specific reason to expect a discontinuous distribution of either emitted or ambient particles, it is unlikely that much larger particles are present in numbers sufficient to dominate the mass of PM-large.

The above conclusions are consistent with an hypothesis that the natural vegetated surfaces which dominate the landscape around the Lake would retain deposited particles more effectively than hard smooth surfaces found in urban areas (where vehicle traffic or other mechanical means of resuspension may be more active). It is expected that deposition and a lack of emission sources over the Lake will result in lower concentrations over the Lake than were observed over land.

4.4.3 Assumptions Presumed to be Bias Neutral

The following assumptions were made as part of the analysis and are intended to support reasonable estimates of the rate of deposition. Though they may introduce a bias, the direction (sign) is not readily apparent.

- Neglecting the effects of particle growth may introduce a small bias. The sign of the bias will depend on particle size. For large and very small particles (< 0.5 μm), this assumption would likely under-estimate deposition rates. For particles in the 0.5 – 1 μm size, deposition rates would be over-estimated. The net effect of this assumption depends on the size distribution of particles at the location.
- Neglecting the effects of breaking waves and spray may introduce a small negative bias. This is developed more fully in section 4.4.
- Aerodynamic roughness length, Z_o , over open water was calculated based upon wind speed as shown in equation (4.9). This is expected to be bias neutral.

4.4.4 Assumptions Introducing a Small Positive Bias in Deposition

The following assumptions are expected to cause a small positive bias in the estimated deposition rates. These biases are thought to be insignificant compared to other uncertainties.

- Small values of aerodynamic resistance calculated in the near-shore zone were suspect. As discussed previously, the basic equations used elsewhere appear to produce invalid results because Z_o is on the same order as the measurement heights. For these cases, the deposition velocity for gases was not allowed to exceed 6 cm/s. Similarly for calculation of the deposition velocity for particles, the value of $1/Ra$ was not allowed to exceed 6 cm/s. The assumption of 6 cm/s is a generous maximum that is likely to allow a positive bias in deposition velocities of gases and particles in the near-shore zone, but it is only applied to a limited area of

the Lake, and only during offshore winds, so the effect on average deposition rates to the Lake is expected to be small.

- Deposition velocities of the gases HNO_3 and NH_3 were approximated as the inverse of the aerodynamic resistance R_a (assumed $R_a \gg R_b$ and $R_c \sim 0$). This is a standard assumption for deposition of very reactive or soluble gases over water (e.g., Valigura, 1995), but may produce a small positive bias in deposition velocity.
- Stability effects were estimated using hourly air and water temperatures with an assumption that air temperature at the water interface equals the water temperature (at 2 cm depth). This assumption is likely to slightly overestimate air temperature at the water interface by an amount likely to vary with wind speeds and season), thereby causing a bias toward less thermal stability, less aerodynamic resistance, and greater deposition velocity than if the actual air temperature were known.
- Increased turbulence due to roughness over land (assumed to be 1 m) was assumed to be advected to 1 kilometer offshore. The deposition velocity in this near-shore zone was calculated as the average of the over-water and near-shore deposition velocities. Calculation of deposition velocity assumed Z_o of 1 m at the shoreline and Z_o as a function of wind speed over open water. This is the arithmetic equivalent of a linear decay from the shoreline deposition velocity to the open water deposition velocity at a distance of 1 km offshore. Thus, for estimation of R_a near the shoreline during periods of offshore winds, an appropriately higher estimate of deposition velocity (than would be provided by the standard over-water formulations) was provided by adjusting Z_o to appropriate values for forested areas. However, the use a Z_o of 1 m caused the maximum deposition velocity to be invoked for the near-shore zone as discussed in the next section. This may result in over estimation of deposition in this region.

The details of the methodology used in this analysis to calculate deposition velocities are shown in Appendix II where the program coding is listed.

4.4.5 Assumptions to be Addressed Further

Dry deposition over water becomes more complicated when strong winds generate breaking waves and spray. The estimated deposition rates presented here do not consider the potential impacts of breaking waves and associated spray. However, because the wind speeds at Tahoe exceed five ms^{-1} only for relatively few hours, the estimated annual deposition rates are expected to be increased only very slightly by inclusion of the effects of breaking waves and spray. Mechanistic modeling of the effects of bubble bursting and spray from whitecap activity upon deposition rates is a research topic in and of itself and is not planned for LTADS. However, an analysis of the potential for breaking waves and spray to increase deposition rates will be included in the final report based upon current literature including the modeling and analytical results of Pryor and Barthelme (2000).

The potential effects of growth of particle size by uptake of water vapor are not quantified in the deposition rates presented here. However, the effects are expected to be insignificant for estimates of the total nitrogen deposition and, at most, a minor influence on particle mass and phosphorus deposition. Most of the nitrogen deposition

is in the gaseous form so particle growth is not expected to make a significant difference in the overall estimates of deposition rates for nitrogen. The deposition of particles in general, and phosphorus-containing particles in particular, could be increased somewhat by hygroscopic growth but that effect is not expected to be large. First, the particles are not necessarily very hygroscopic. Second, the amount of growth before deposition occurs may be minimal. Early modeling of particle growth (Williams, 1982) assumed equilibrium between water vapor and aerosols. However, Zufall et al. (1998) concluded that particles larger than 0.1μ do not reach equilibrium before depositing and showed that models assuming equilibrium can overestimate the effects of hygroscopic growth on deposition by as much as a factor of 5. Hygroscopic particle growth may affect deposition rates positively or negatively in amounts that depend on the environmental conditions and the chemical composition and initial size of the particles. Using alternative models that do not assume equilibrium, Pryor, et al. (2000) indicated hygroscopic growth may increase the deposition rate significantly for highly hygroscopic particles in the size range of $D_p \sim 0.3-10 \mu$, but the particles observed in LTADS are primarily comprised of less hygroscopic constituents. The size of NH_4NO_3 aerosol is likely $D_p \sim 0.3-6 \mu$ but NH_4NO_3 is only expected to contribute a very minor amount of the N load compared to gaseous HNO_3 and NH_3 . For $D_p < 0.3 \mu$ and moderate wind speeds ($U < 10 \text{ m/s}$), particle growth is expected to decrease Brownian diffusion, thus increasing R_d and thereby decreasing V_d . For $D_p > 10 \mu$ the effect of hygroscopic growth is to increase impaction and V_g but the relative change in deposition velocity is less. At higher wind speeds, the viscous layer is thinner and inertial impaction acts more effectively so that particles deposit more quickly and the effects of particle growth are minimal.

The current formulations for deposition rate are theoretically applicable to smooth surfaces (although they are commonly used in boundary layer meteorology). The final report will include a brief review of available information on the formulations of R_a appropriate for use with rough surfaces.

The amounts by which concentrations differ between the lakeshore and mid-lake (and the amount by which deposition rates are likely overestimated) is not considered in the conservative deposition estimate presented here. The concentration differences will depend upon the depth of vertical mixing and the ambient concentrations above and below the top of the mixed layer, which will vary in height. The vertical extent of mixing will generally differ over the Lake from that over land and those differences will vary with season and time of day. For the final report, using LTADS observations and a range of assumptions, we expect to make bounding calculations to estimate the differences between mid-lake and shoreline mass concentrations and deposition rates. Assumptions will be necessary to characterize concentrations aloft because resources (and in some cases methods) were not available to make vertically resolved measurements of concentrations.

4.5 Variations in Deposition Velocity

The deposition velocities calculated from the meteorological data in this analysis exhibited significant temporal variation as well as spatial variation between near-shore

and open-water areas. The significant temporal variation in calculated deposition velocities was associated mainly with the daily variation in wind speed and direction. In contrast, relatively small differences were found between the seasonally averaged deposition velocities calculated from meteorological data representing different sites.

Deposition velocities calculated for open-water areas were equal to those for the near-shore zone during periods when the wind direction was from the Lake toward the shore (onshore) due to use of the same (over water) roughness length. In the near-shore zone, the seasonally averaged deposition velocities were larger by about an order of magnitude compared to those for the open water areas. The deposition velocities for open-water areas also varied by an order of magnitude due primarily to changes in wind speed.

Table 4.1 displays estimates of the annual averaged deposition velocities for three sites. Deposition velocities for gases are followed by deposition velocities for characteristic particle sizes grouped according to the assumptions for the lower bound (1, 5, 15 μm), best (2, 8, 20 μm), and upper bound (2.5, 10, 25 μm) estimates. Estimates are shown for the weighted average of near-shore and mid-Lake areas, and for these areas individually. The composite deposition velocity for the Lake as a whole is simply a weighted average of the near-shore and mid-Lake areas (assumed to be 20 and 80 percent respectively). The deposition velocities for mid-Lake areas are presumed to be the more reliable numbers and the estimates for the near-shore areas are about 10 times larger. These larger estimates for the near-shore zone are a consequence of the sensitivity of the equations to the aerodynamic roughness length where observation height is less than $50 Z_o$ and the somewhat arbitrary assumption of the very conservative capping value of 10 cm/s for $1/R_a$ used for the upper bound estimate of deposition velocity. The capping values for $1/R_a$ of 3, 6 and 10 cm/s used for the lower bound, best, and upper bound estimates of deposition velocities and subsequent deposition rates, were applied in the calculations for both gases and particles.

The annual averages are the simple average of the seasonal average values. Seasonal averages are calculated based upon the hours within each three month season for which data is reported. The U.S. Coast Guard pier site operated in all four seasons, however, Buoy TDR2 did not report data for any of the winter months and Timber Cove reported no data for the spring months. Thus differences in wind speeds and estimated deposition velocities between SE Buoy TDR2 and Timber Cove may be due to these sites seasonal differences in data recovery.

Table 4.1 Comparison of annual average deposition velocities estimated based upon meteorological observations from three sites (with the assumption that 1/Ra is capped at a maximum of 6 cm/s). Differences in wind speeds and estimated deposition velocities between SE Buoy TDR2 and Timber Cove are due in large part to their seasonal differences in data recovery.

Sites		US Coast Guard Pier				SE Buoy, TDR2				Timber Cove			
Gas or PM-size	Characteristic Particle Diameter	Wind Speed (m/s)	Deposition Velocities (cm/s)			Wind Speed (m/s)	Deposition Velocities (cm/s)			Wind Speed (m/s)	Deposition Velocities (cm/s)		
			Composite	Near-shore	Mid-Lake		Composite	Near-shore	Mid-Lake		Composite	Near-shore	Mid-Lake
Gases	N/A	2.9	0.8	2.1	0.5	2.9	0.8	1.9	0.5	3.1	0.8	2.2	0.4
PM-Fine	1.0		0.3	1.1	0.1		0.2	0.8	0.1		0.2	0.8	0.1
PM-Coarse	5.0		0.3	1.1	0.2		0.3	0.9	0.2		0.3	0.9	0.2
PM-Large	15.0		0.9	1.6	0.7		0.9	1.4	0.7		0.9	1.4	0.7
PM-Fine	2.0		0.3	1.1	0.1		0.3	0.9	0.1		0.2	0.8	0.1
PM-Coarse	8.0		0.5	1.2	0.3		0.4	1.0	0.3		0.4	1.0	0.3
PM-Large	20.0		1.4	2.1	1.2		1.4	1.9	1.3		1.4	1.8	1.2
PM-Fine	2.5		0.3	1.1	0.1		0.3	0.9	0.1		0.2	0.8	0.1
PM-Coarse	10.0		0.6	1.3	0.4		0.5	1.1	0.4		0.5	1.0	0.4
PM-Large	25.0		2.1	2.7	1.9		2.0	2.5	1.9		2.0	2.5	1.9